Available online at www.sciencedirect.com
SCIENCE @ DIRECT®
Combustion and Flame 146 (2006) 168–179
Combustion and Flame
www.elsevier.com/locate/combustflame

The propagation of tribrachial flames in a confined channel

Nam Il Kim [a,*], Jeong Il Seo [b], Young Tae Guahk [b], Hyun Dong Shin [b]

[a] *School of Mechanical Engineering, Chung-Ang University, Heukseok-dong, Dongjak-gu, Seoul 156-756, Republic of Korea*
[b] *Department of Mechanical Engineering, Korea Advanced Institute of Science and Technology, 373-1 Guseong, Yuseong, Daejeon 305-701, Republic of Korea*

Received 10 July 2005; received in revised form 23 March 2006; accepted 2 April 2006

Available online 11 May 2006

Abstract

A flame formulated in a mixing layer has a typical structure of a tribrachial (or triple) flame. The propagation velocity of a tribrachial flame is much higher than the laminar burning velocity of a stoichiometric premixed flame, and the propagation velocity usually decreases as the gradient of fuel concentration increases. A separate experimental study that used a jet flow in an open space reported that there is a maximum propagation velocity at a critical fuel concentration gradient coupled with the enhancement of a diffusion flame branch and that the critical concentration gradient can be varied even by the difference in velocity variation near the flame. This study investigates how a confined flow field affects the structure of a tribrachial flame. The mean velocity and the concentration gradient of fuel were controlled by a multislot burner. Laser diagnostic methods were used to measure the velocity variation, the OH radical, and the temperature variation. Even in a confined geometrical space, the existence of the maximum propagation velocity was confirmed. Moreover, the critical concentration gradients in a confined channel were larger than those in an open jet case; that is, the role of the diffusion flame at the maximum propagation velocity becomes more significant in a confined structure due to the enhanced convective diffusion. This result shows the importance of the diffusion branch in a confined (or squeezed) stream tube.

© 2006 The Combustion Institute. Published by Elsevier Inc. All rights reserved.

Keywords: Tribrachial flame; Triple flame; Propagation velocity; Flame stabilization; Concentration gradient

1. Introduction

A tribrachial (or triple) flame can form in a mass diffusive mixing layer with a flammable concentration. The tribrachial flame consists of a lean premixed flame, a rich premixed flame, and a diffusion (or nonpremixed) flame. The junction of the three reaction branches is called a tribrachial point. This structure was first reported by Phillips [1], who experimented on flame propagation in a horizontal methane–air stratified mixing layer in order to simulate mine explosions. Phillips showed that the propagation velocity of a tribrachial flame (PVTF), or V_f, is much larger than the laminar burning velocity of a stoichiometric mixture. Ishikawa [2] observed similar flame structures through experiments on the transient flames that formed in a stratified methane–air layer in a chamber with constant volume. In an analytical study, Dold [3] recognized the importance of the tribrachial flame for turbulent modeling.

A number of studies have since been conducted on the tribrachial flame, especially with regard to the

---

[*] Corresponding author. Fax: +82 2 814 9476.
E-mail address: nikim@cau.ac.kr (N.I. Kim).

0010-2180/$ – see front matter © 2006 The Combustion Institute. Published by Elsevier Inc. All rights reserved.
doi:10.1016/j.combustflame.2006.04.001

dependency of the PVTF on the gradient of the fuel's mass fraction (or *concentration gradient*), which is an important issue. Although Phillips reported that the propagation velocity decreases as the mixing thickness decreases, the concentration gradient was not quantitatively evaluated.

Kioni et al. [4] connected a multislot burner to a slightly diverging channel and strictly controlled the concentration gradient of methane. They used diluted methane (with 55% N_2), and their results also showed that the propagation velocity of the tribrachial flame was much larger than the laminar burning velocity. However, the propagation velocity in their experiment increased slightly as the concentration gradient increased. The discrepancy in the correlation between the PVTF and the concentration gradient has been attributed to the confined geometry of the channel.

Ruetsch et al. [5] analytically explained that the ratio of the PVTF to the laminar burning velocity of a stoichiometric mixture asymptotically converges to the square root of the density ratio of the unburned mixture to the burned mixture when the concentration gradient approaches a very weak concentration gradient. They expressed the ratio as

$$V_\mathrm{f} \sim S_\mathrm{L}^0 \sqrt{\rho_\mathrm{u}/\rho_\mathrm{b}}, \tag{1}$$

where S_L^0 is the laminar burning velocity of the stoichiometric mixture, ρ_u is the density of the unburned mixture, and ρ_b is the density of the burned mixture. Their results are extremely valuable in terms of understanding the characteristics of typical tribrachial flames. They explained the mechanism of the increase in the PVTF in terms of the upstream flow redirection, which is due to the volume expansion near the tribrachial point [5,6].

The approach of Chung and his research group [7–10] revealed that the base of a lifted diffusion flame can be explained by the structure of the tribrachial flame and helped to explain the essential mechanism of turbulent lift-off flames. To measure the PVTF, Ko and Chung [9] used the propagating flames of a small diffusion jet and relied on analytical results derived from a boundary layer theory. Their PVTF was much higher than the laminar burning velocity and it decreased as the concentration gradient increased. This result agrees well qualitatively with the estimate by Ruetsch et al. with regard to the limit of small concentration gradient. However, the ultimate state of a zero concentration gradient needs to be reconsidered. If the concentration gradient becomes zero, then the mixture becomes a well-premixed gas. Thus, the flame in such a mixture becomes a premixed flame—not a tribrachial flame. The propagation velocity of the premixed flame must then be of the same order as the laminar burning velocity, which is much smaller than the value asymptotically estimated by Ruetsch et al. [5].

Discrepancy between the PVTF and the concentration gradient motivated the study of Kim et al. [11]. They were the first to investigate a tribrachial flame stabilized in a potential core of a large jet in an open space (that is, an open jet). Under such conditions, a unique mechanism of flame stabilization is the flow redirection caused by the flame itself. This mechanism is the main reason for the increase in the PVTF. In addition, the lift-off heights were sensitive to the *mean velocity* and the concentration gradient. Thus, the blow-off conditions of a tribrachial flame with an open jet, which were defined as the maximum velocity for flame stabilization, could be a good method for measuring the PVTF. Kim et al. [11] showed that there is a *critical concentration gradient* at which the PVTF reaches its maximum. They suggested three causes: the limitation of the burner, the nonuniform velocity profiles, and the additional volume expansion by the diffusion flame.

Briefly, the limitation of the burner implies that when the size of the burner is not sufficient to establish an "ideal tribrachial flame," the flame edges close to the flammable limits are eliminated and the overall propagation velocity of the tribrachial flame is underestimated. Here, the ideal tribrachial flame is defined as a tribrachial flame that has been stabilized in an infinite uniform velocity field with linear concentration profiles that cover all flammable conditions from the lean limit to the rich limit [11].

According to the results of Kim et al. [11], this critical concentration gradient varied when the flame was near the nozzle's exit. This result raised questions about the effect of the flow deflection on the characteristics of the tribrachial flame. In regard to this, the differences between the theoretical tribrachial flame and the flame in the confined channel have not yet been clarified, even though confined channels have often been used in this research field. Furthermore, neither the difference between the planar mixing layer and the round jet nor the effect of the shear layer has been distinguished clearly. We therefore investigated the tribrachial flames in a slightly diverging channel as the first step in elaborating the effect of the velocity field. In such a channel, flow divergence is expected to be suppressed and the concentration gradient maintained at a higher level, resulting in enhanced mass diffusion, especially behind premixed flame branches.

Our two primary objectives were to investigate whether a tribrachial flame in a slightly diverging channel has a critical concentration gradient for the maximum PVTF as observed in the open jet and to explain the difference between a tribrachial flame that has stabilized in an open jet and one in a confined channel. To experimentally investigate the PVTF and the structure of the flame, we used various laser diagnostic techniques, the results of which can expand our understanding of the characteristics of the tribrachial flame.

2. Experimental method

We used methane (with a purity of 99.95%) and propane (with a purity of 98%). Fig. 1 shows the test section with a slightly diverging channel. The diverging angle of the channel was set to 3.5° on each side, which is the same angle chosen by Kioni et al. [4]. We connected a multislot burner with a contraction nozzle to the diverging channel and named the starting point of the channel the *nozzle exit*. Details of the burner have been presented elsewhere [11]. Fig. 1 shows the coordinates for the direction of the flow (x), the concentration gradient (y), and the depth (z).

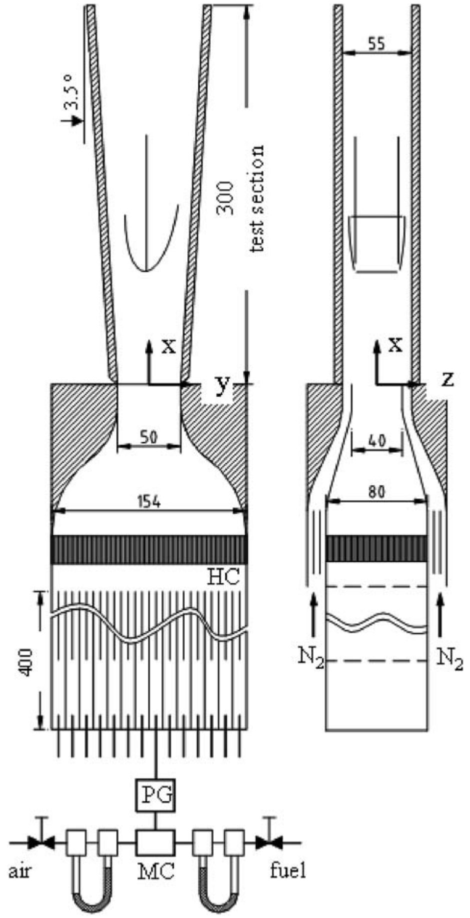

Fig. 1. Experimental apparatus (HC: honeycomb, PG: particle generator, MC: mixing chamber, length unit is mm).

Our two experimental parameters were the *mean velocity* and the *concentration gradient* (that is, the gradient of the fuel's mass fraction). There were 14 slots in the y-direction for the premixed mixtures and two additional slots for the side nitrogen in the z-direction. By adjusting the flow rate and the equivalence ratio of the mixture in each slot, we could strictly control the overall flow rate and the concentration gradient.

The effects of side nitrogen layers were examined by varying the flow rate of the nitrogen. As a result, even though a small deviation was found for the lift-off heights of the flames, the overall trends were similar regardless of the flow rate. Thus, the mean flow velocity of the nitrogen was regulated such that it had the same mean velocity as the main stream of the mixture. All flame shapes then had negligible deviation in the z-direction compared with the flame width and the scale of experimental fluctuation in the lift-off heights. Thus, all flames in this study were considered to be two-dimensional structures.

For the luminous intensities of the tribrachial flames, we used an intensified CCD camera. The maximum intensity was obtained near the tribrachial point. The lift-off height was defined as the distance between the nozzle exit and the location of the maximum luminous intensity. To measure the lift-off heights, we averaged more than a hundred images.

A hot-wire anemometer (Dantec CTA56C17) was used to measure the velocity of the cold flow, and a particle image velocimeter (PIV) was used to measure the velocity of the reacting flow. We also used a double pulse Nd:YAG laser (500 mJ, 532 nm) with a pulse interval of 224.9 µs. We installed a 532-nm bandpass filter (with a bandwidth of 10 nm) to exclude the flame luminosity. The seed particle was 0.5 µm of Al_2O_3. The concentration gradient of the methane was measured with the aid of mass spectroscopy (HIDEN HPR20).

To detect OH radicals, planar laser-induced fluorescence (PLIF) techniques were used. The laser pulse was generated by a second harmonic Nd:YAG laser (500 mJ, 532 nm), and a pumped dye laser with a frequency doubler was tuned to 283 nm with a pulse energy of 12 mJ. An intensified CCD camera (512 pixels × 512 pixels) was equipped with an FG-09 filter and an FG-01 filter.

For the temperature, the shapes of the coherent anti-Stokes Raman scattering (CARS) spectra of nitrogen were used. The spectra were taken with a monochrometer equipped with another intensified CCD camera (1024 pixels × 256 pixels) over a Raman shift frequency range of 2260 to 2350 cm^{-1}. For that, we used a single-mode Nd:YAG laser (532 nm) to generate a pump laser and a modeless dye laser to generate a Stokes laser [12].

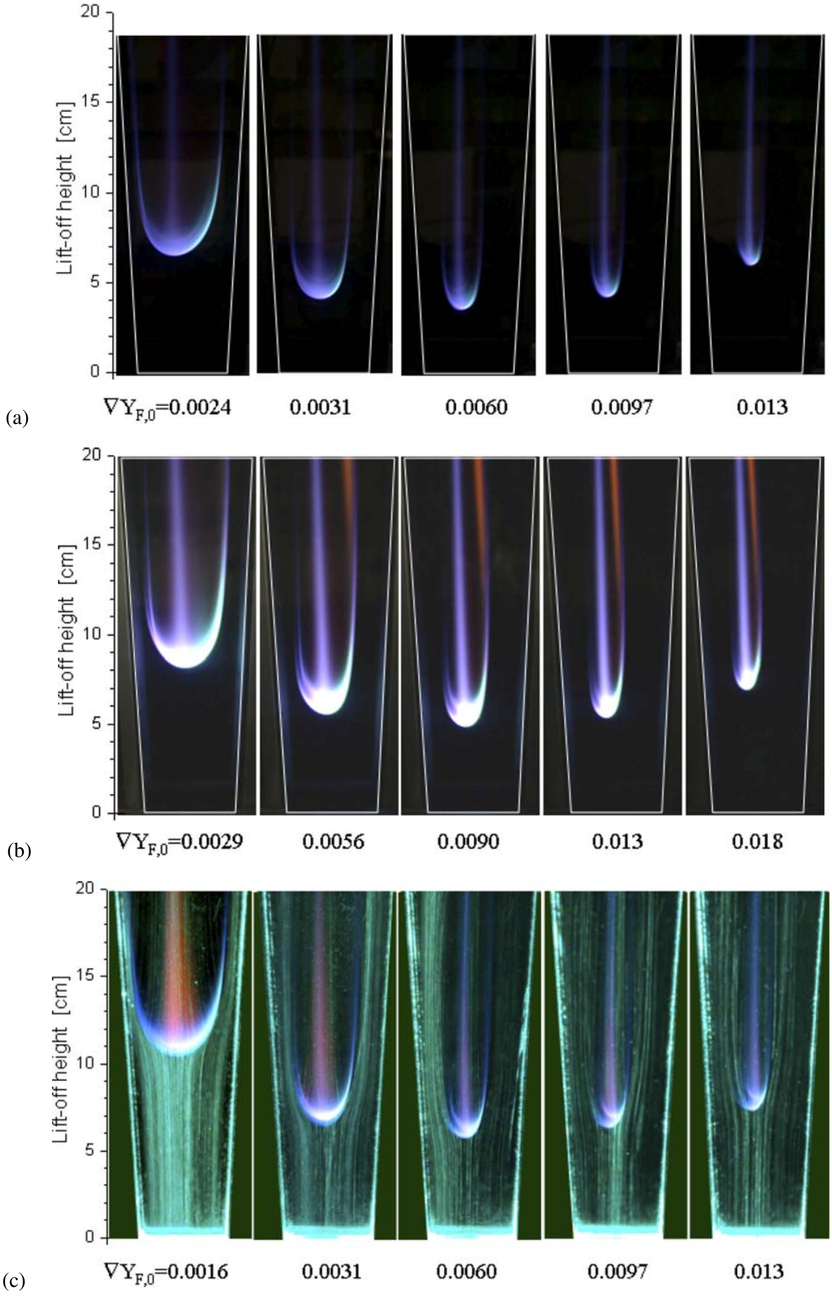

Fig. 2. Photographs of tribrachial flames: (a) direct images of a methane flame, $V_{\mathrm{m},0} = 102.5$ cm/s; (b) direct images of a propane flame, $V_{\mathrm{m},0} = 120$ cm/s; (c) visualization of streak lines (methane, $V_{\mathrm{m},0} = 105$ cm/s).

3. Results and discussion

3.1. Flame shapes and lift-off heights

Fig. 2 shows direct images of the tribrachial flames with the concentration gradients for fixed mean velocities. The concentration gradient at the nozzle exit, $\nabla Y_{\mathrm{F},0}$, was measured, and the mean velocity at the nozzle exit, $V_{\mathrm{m},0}$, was defined as the flow rate divided by the cross-sectional area of the channel at the nozzle exit. Figs. 2a–2c show images of the methane flames and propane flames, as well as the Mie-scattering images of the streamlines near the methane flames. In all results of this study, the left-hand side was fuel-lean and the right-hand side was fuel-rich. As the concentration gradient increased, minimum lift-

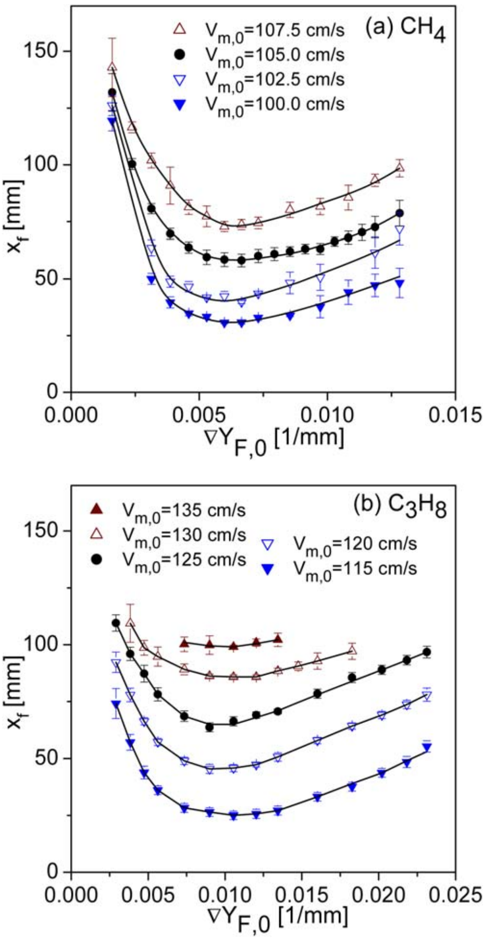

Fig. 3. Variation of the lift-off height with the concentration gradient at the nozzle exit and the mean velocity at the nozzle exit for (a) methane and (b) propane.

off heights existed for fixed mean velocities, and the width of the premixed flame branch in the y-direction decreased to less than the width of the channel. Thus, the curvature of the flame was enlarged as much in an open jet, and the luminous intensity of the diffusion flame was also stronger than that of an open jet, even for a concentration gradient smaller than the critical gradient. The streamlines near the flame in Fig. 2c show that the flow divergence is significantly restricted when the concentration gradient is small (compare with Fig. 4c in [11]). The flame position was noticeably disturbed with particle seeding, and the images in Fig. 2c were chosen when the disturbances were small.

The variation in the lift-off height with the concentration gradient is shown in Fig. 3a for the methane flames and in Fig. 3b for the propane flames. As the concentration gradient increased, the lift-off height decreased and then increased, depending on the concentration gradient. Lift-off heights reached a minimum value at the critical concentration gradient. Compared with flames that stabilize in an open jet [11], flames in a channel stabilized more easily, since flame stabilization can be obtained even with much higher mean velocities or at greater lift-off heights. Moreover, for the same variation of the concentration gradient, the resultant variation of the lift-off heights was much smaller than that in the open-jet case. As a result, blow-off was not observed under the experimental conditions of this study, although it could readily be observed in the open jet experiment [11].

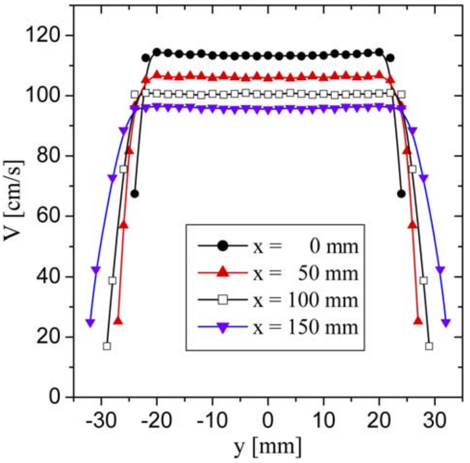

Fig. 4. Velocity distribution of a nonreactive flow in the channel ($V_{m,0} = 100$ cm/s).

3.2. Definition of the mean velocity and the concentration gradient

The essential differences of a flow in a confined channel are the variation in velocity and the concentration gradient of the nonreactive flow. We measured the velocity distribution of a nonreactive flow using a hot-wire anemometer in the channel. Fig. 4 shows the results. We found that uniform velocity profiles were maintained near the center. However, the width of the uniform velocity grew slightly as the height increased but the mean velocity decreased inversely. This phenomenon is mainly due to the conservation of the total flow rate and the increase in the cross-sectional area of the channel. Although these results are not novel, the trend and the relation to the concentration gradient should be checked in order to validate the experimental limits and characteristics.

The depth of the channel in the z-direction was 55 mm, and the width of the channel in the y-direction can be written as $W(x) = W_0 + 2x \tan\theta$, where W_0 is the channel width at the nozzle exit ($W_0 = 50$ mm) and θ is the slope angle of the wall ($\theta = 3.5°$). The *ideal mean velocity*, $V_{\mathrm{m},x}$, can then be written

$$V_{\mathrm{m},x} = V_{\mathrm{m},0} W_0 / (W_0 + 2x \tan\theta), \tag{2}$$

where $V_{\mathrm{m},0}$ is the mean velocity at the nozzle exit. Instead of using the measured velocity at the center, we obtained the mean velocity at the nozzle exit, $V_{\mathrm{m},0}$, from the ratio of the flow rate to the cross-sectional area. This definition is more reasonable because the total flow rate is conserved in the channel regardless of the existence of the flame. Such a definition is also close to the physical meaning of the propagation velocity of a premixed flame in a confined channel. An additional strength is that the same definitions have been used as representative velocities in previous studies conducted in channels or in open jets [1,4,11,13].

Fig. 5 plots the variation of the ideal mean velocity and the measured velocity at the center of the cross-sectional area, and the results are compared with the experimental results for the open jet [11]. All the results have the same flow rate of the mean velocity of 100 cm/s at the nozzle exit. The axial mean velocity in the channel decreases with the height, while the axial mean velocity of the open jet is almost constant. The measured velocity at the nozzle exit is 1.14 times the ideal mean velocity estimated from the flow rate. Even though the measured velocity in the channel is similar to the ideal case in their trends, the deviation between the experimental and ideal velocities increases in the direction of the stream, probably due to the growth of the shear layer near the wall.

As with the velocity variation, the concentration gradient also varies in the direction of the stream, generally by two mechanisms: the convective diffusion due to the diverging flow field and the mass diffusion due to the concentration gradient. However, variation in the concentration gradient by the mass diffusion is negligible since the concentration gradient is constant within the area of interest in which flames are formulated; i.e., the derivative of the constant concentration gradient is zero. By assuming that the fuel concentration of each stream line is maintained, the *ideal concentration gradient* can then be written

$$\nabla Y_{\mathrm{F},x} = \nabla Y_{\mathrm{F},0} W_0 / (W_0 + 2x \tan\theta), \tag{3}$$

where $\nabla Y_{\mathrm{F},0}$ is the concentration gradient at the inlet of the channel. We used the measured concentration gradient at the nozzle exit, $\nabla Y_{\mathrm{F},0}$, as the initial concentration gradient on the basis of Eq. (3). The local concentration gradient, $\nabla Y_{\mathrm{F,f}}$, was estimated at the tribrachial position x_{f}. As a result, we found that the dependency of the concentration gradient on the mean velocity was negligible under our experimental conditions because the residence time in the test section was sufficiently short compared with the diffusion time scale of a cold mixture across the channel under the weak concentration gradient in this experiment.

The second mechanism of mass diffusion is not significant because a linear distribution of species does not cause a change in the local flux. Only an overall shift in concentration may occur from the rich side to the lean side with the order of the characteristic diffusion length $(D_{\mathrm{u}}\tau_c)^{0.5}$, where D_{u} is the mass diffusivity of the unburned mixture and τ_c is a convective time scale. The mass diffusivity of the unburned mixture was on the order of 10^{-5} m^2/s. The convective time scale was less than 10^{-1} s based on the length of the test section and the mean velocity. The characteristic diffusion length is subsequently on the order of 10^{-3} m, which is negligible compared with the spatial resolution of this experiment.

However, the mass diffusion becomes significant when the concentration profile has a stepwise distribution; that is, the concentration of the rich side has a finite value and there is a drastic variation between the lean and rich sides near the stoichiometry. This situation may occur when a small number of slots are connected directly to the channel, as often adopted in other experiments. The concentration gradient then decreases from an infinitely large value to a small value; moreover, it does not depend on the cross-sectional area of the channel but on the diffusion velocity. Under such experimental conditions, as opposed to those of the present study, the variation of the local concentration gradient along the stream should therefore be evaluated in conjunction with the increase in the mixing thickness of the species.

As shown in Fig. 6, we used mass spectroscopy to evaluate the concentration gradient of the methane–air mixture without flame along the stoichiometry line. The trend in the experimental results is similar to the trend in the ideal concentration gradient of

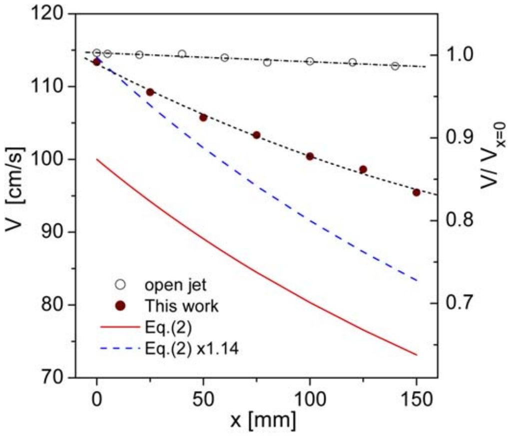

Fig. 5. Variation of the velocity of a nonreactive flow in the axial direction ($V_{\mathrm{m},0} = 100$ cm/s).

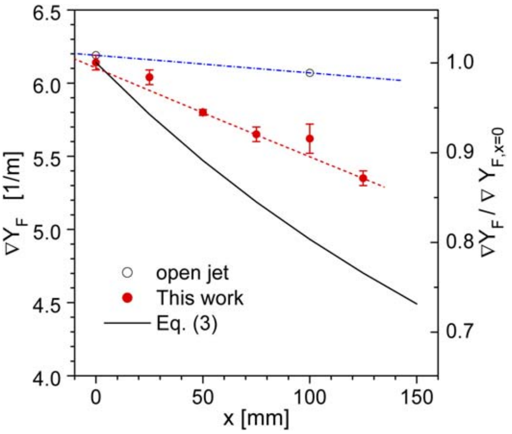

Fig. 6. Variation of the concentration gradient of a nonreactive flow in the axial direction ($V_{m,0} = 100$ cm/s).

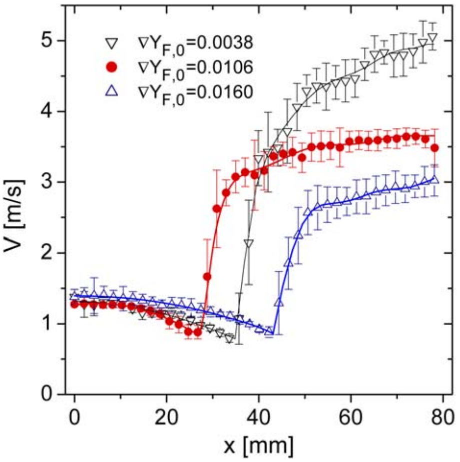

Fig. 7. Velocity variation in the direction of the stream, as measured by the PIV method (propane, $V_{m,0} = 120$ cm/s).

Eq. (3). Moreover, as with the velocity variation in Fig. 5, the deviation between the ideal concentration gradient and the measured results increases in a similar trend with the height.

3.3. Propagation velocity

When there is a flame in the channel, the velocity field near the flame is deflected. The velocity distribution near the flame was measured with the PIV method and the results are shown in Fig. 7. Along the same line of height, the minimum velocity was plotted at the upstream, while the maximum velocity was plotted at the downstream. The velocity decreases slightly at the nozzle exit and then decreases steeply in front of the thermal layer. The minimum velocity in front of the flame is known to be in the same order as the laminar burning velocity [5]. For detailed study of the local burning velocity, measurement with high resolution is required in front of the thermal layer, but this task is beyond the scope of this study.

Across the premixed flame, the velocity increases drastically due to thermal expansion. However, behind the premixed flame, the velocity continually increases. This likely can be attributed to the additional volume expansion from the curved surfaces of the premixed flame downstream from the tribrachial point, or from the diffusive reaction behind the premixed branch. In a confined geometry, the volume source generates velocity increases in the direction of the stream, as with a flame in a tube. When the concentration gradient is small, the curved premixed flame lengthens in conjunction with the enlarged overall scale of the flame. Thus, the velocity behind the premixed flame accelerates with the continuous heat release from the flame. Another effect is concerned with the development of the flow. The velocity field which has been already disturbed by the flame develops to a new velocity field in the channel, and it increases the velocity along the stream at the center of the cross-sectional area coupled with the increase of the viscosity of the burned gas. In addition, as a minor reason, a small portion of the continuous increase in velocity may also be attributable to the buoyancy effect.

Even though the ideal mean velocity and the ideal concentration gradient do not correspond with the real velocity and the real concentration gradient, they can be representative values coupled with the strong similarity between the mean velocity and the concentration gradient. Thus, the lift-off height, x_f, was converted to the PVTF, V_f, against the concentration gradient, which is based on Eqs. (2) and (3). Fig. 8a shows the results for the methane flames, and Fig. 8b shows the results for the propane flames. All the experimental results agree well with each other, and the critical concentration gradients were 0.0054 for methane and 0.0085 for propane. These values are about twice the values of the critical concentration gradients, which we obtained from the blow-off conditions of the open jet experiment: 0.0025 for the methane and 0.0047 for the propane [11].

Fig. 9 compares the PVTF in this study with the flame stabilization conditions of the open jet experiment, along with other relevant measurements. In the open jet experiment, the blow-off conditions were suitable for measuring the PVTF. Thus, the extrapolated line of the blow-off conditions agreed fairly well with the analytical value, MA, for a zero concentration gradient, especially in the case of methane [5]. The results of Ko and Chung [9] were smaller than the analytical value MA. Furthermore, the results by Kioni et al. [4] present quite a different trend, which will be explained later. One notable result is that even

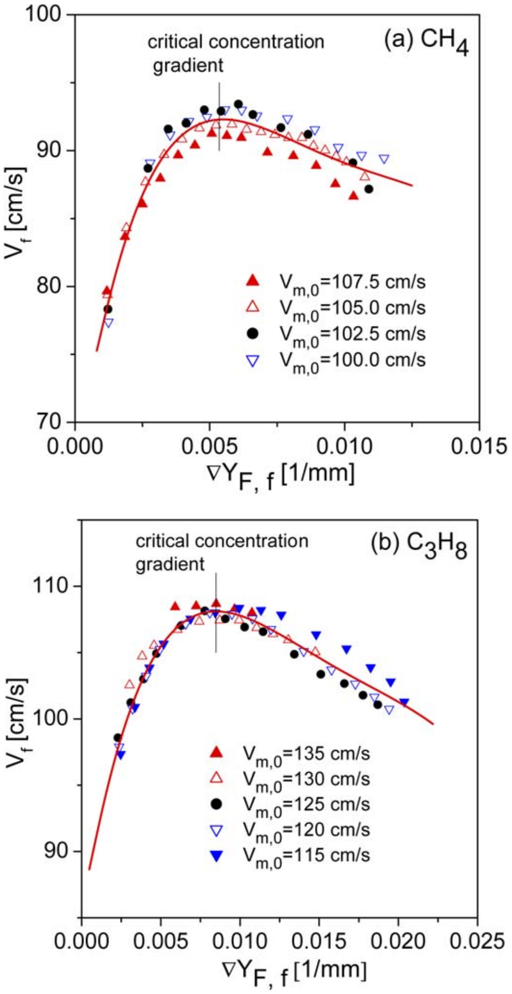

Fig. 8. Propagation velocity with the concentration gradient for (a) methane and (b) propane.

in the open jet, the critical concentration gradient shifted to higher values as the flame approached the nozzle exit, and the values were close to the critical concentration gradients of the present experiment. In conclusion, the PVTF of the flame in the channel is close to the results of the flashback in the open jet, which was defined as the condition whereupon the flame base moves into the contraction nozzle.

Even in the case of the open jet, the flow divergence near the nozzle exit is restricted by the contraction nozzle. Thus, the flow situation near the nozzle exit is similar to the flow in the channel. From these results, we can extend the discussion on the flame in a confined channel to the situation where the flow divergence by the flame is partially suppressed due to the external flow around the flame. For example, if there were an additional coaxial flow around the open jet, the flow divergence near the flame in the open jet might be equally restricted. We can then expect the propagation velocity to decrease as it does in the channel or near the nozzle. Based on these results, it is believed that the task of measuring the PVTF with an open potential jet is the most reasonable among all experimental methods that have been suggested thus far, because it is less affected by the given velocity disturbance by a confined channel or shear layer.

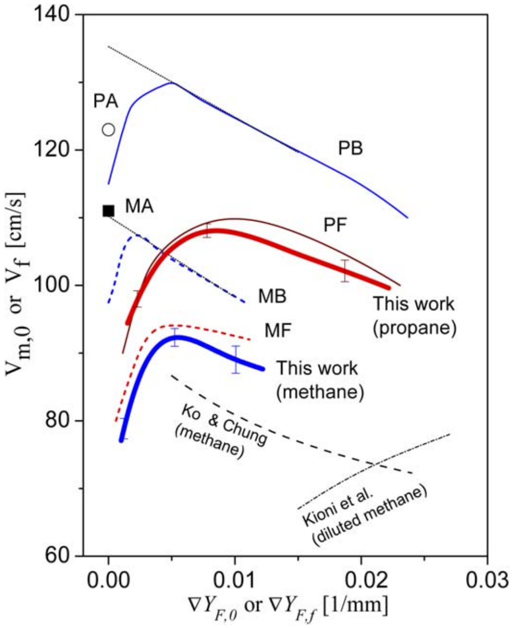

Fig. 9. Comparison of the propagation velocities of propane and methane flames in a channel with other results. PA: the analytic value of a propane flame [5]; PB: the mean velocity for the blow-off of a propane flame [11]; PF: the mean velocity for the flashback of a propane flame [11]; MA: the analytic value of a methane flame [5]; MB: the mean velocity for the blow-off of a methane flame; MF: the mean velocity for the flashback of a methane flame; Ko and Chung [9]; Kioni et al. [4].

Before investigating the reason for the maximum PVTF, we will briefly discuss flame stabilization from the viewpoint of the response of the PVTF to the concentration gradient. When the mean velocity is matched to the propagation velocity, a stationary flame is obtained. Considering a slight disturbance in the flame position, ε, we can express the variation of the mean velocity and the concentration gradient from Eqs. (2) and (3) as follows:

$$\frac{\nabla Y_{\mathrm{F},x+\varepsilon}}{\nabla Y_{\mathrm{F},x}} = \frac{V_{\mathrm{m},x+\varepsilon}}{V_{\mathrm{m},x}}. \tag{4}$$

To estimate the sensitivity of the propagation velocity to the disturbance of the concentration gradient, the PVTF, V_f, was presented as being proportional to the concentration gradient to the power of a as follows:

$$\frac{V_{\mathrm{f},x+\varepsilon}}{V_{\mathrm{f},x}} = \left(\frac{\nabla Y_{\mathrm{F},x+\varepsilon}}{\nabla Y_{\mathrm{F},x}}\right)^a = \left(\frac{V_{\mathrm{m},x+\varepsilon}}{V_{\mathrm{m},x}}\right)^a. \tag{5}$$

The response rate a becomes a function of the concentration gradient and determines how the propagation velocity responds to the concentration gradient. A flame slightly disturbed upstream ($\varepsilon < 0$) confronts an increased mean velocity and its propagation velocity decreases inversely if a is negative. In most of the literature, a is negative. The flame then moves downstream, resulting in a stable flame. That is, the variation in the PVTF is smaller than that of the mean velocity caused by a perturbed distance. Thus, the variation in the lift-off heights is small when the concentration gradient is larger than the critical value as shown in Fig. 3.

If a is positive, on the other hand, there is an increase in the propagation velocity of a flame that is slightly disturbed upstream. Consequently, the response of the flame is more sensitive than when a is negative. Furthermore, if a is greater than unity, the flame will become unstable because the increase in the propagation velocity may be larger than the increase in the mean velocity; i.e., the flame slightly disturbed upstream propagates farther upstream, and the flame propagation cannot be prevented by the increase in the mean velocity. When the disturbance, ε, becomes infinitely small, the response rate can be written as follows:

$$a = \frac{d(\ln V_\mathrm{f})}{d(\ln \nabla Y_{\mathrm{F},f})} = \frac{\nabla Y_{\mathrm{F,f}}}{V_\mathrm{f}} \frac{dV_\mathrm{f}}{d\nabla Y_{\mathrm{F,f}}}. \tag{6}$$

Fig. 10 shows the response rates for the propane and methane flames. We used the fitting lines of the propagation velocity in Fig. 8 for Eq. (6). The response rates are much smaller than unity for all experimental results. Thus, the tribrachial flames can be stabilized in a channel regardless of the sign of a. In the overall trend, the response rates decrease as the concentration gradient increases, and the variation in the response rates becomes small.

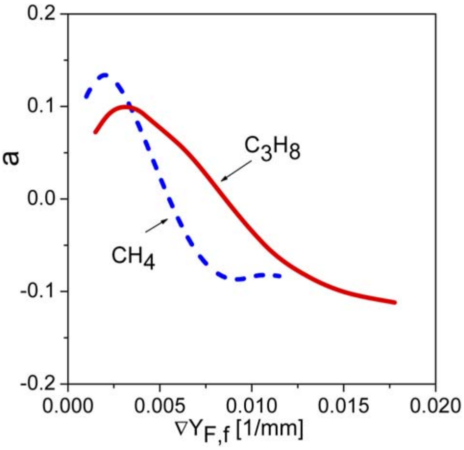

Fig. 10. Response rate of the propagation velocity with the concentration gradient.

3.4. Structure

The existence of the maximum PVTF is important in combustion study because it can be a bridge or a criterion between a premixed flame and a typical tribrachial flame. With respect to the reason for the existence of the maximum PVTF, three mechanisms, the limitation of the burner, the effect of nonuniform velocity profiles, and the effect of the diffusion flame, have been introduced [11]. It was also shown that the ambiguities arising from the previous two mechanisms with respect to the limitation of the burner and the effect of nonuniform velocity profiles can be eliminated by employing a clearer definition of an "*ideal tribrachial flame*" [11]. However, the third mechanism, namely the effect of the diffusion flame, concerns the additional volume expansion by the reaction at the diffusion branch, especially near the premixed flame branch [11].

In this study, however, the flame is located in a channel and the ideal tribrachial flame is not available. Thus, the third mechanism was investigated mainly in conjunction with the second mechanism. That is, we expected the confined structure to enlarge the convective diffusion, thereby manifesting the maximum PVTF. Although more studies are needed to clarify the effects of diffusion on the PVTF, the following three points should be first confirmed so as to validate the possible contribution by the additional reaction along the diffusion flame to the PVTF:

- The experimental method must be sufficiently sensible to detect a small variation in the PVTF.
- The reaction rate of the diffusion branch must be enhanced in relation to the reaction rate of the premixed flame when the concentration gradient is under the critical value.
- The temperature variation along the diffusion branch must be capable of indicating any additional heat release.

First, we relied on Fig. 3 to estimate the experimental resolution of the lift-off height. Near the critical concentration gradient, the deviation of the lift-off heights between the two different mean velocities of 102.5 and 105.0 cm/s was about 18 mm for the methane flames. In addition, the standard deviation of the measured lift-off height was less than 3 mm under the same conditions. Thus, the experimental has res-

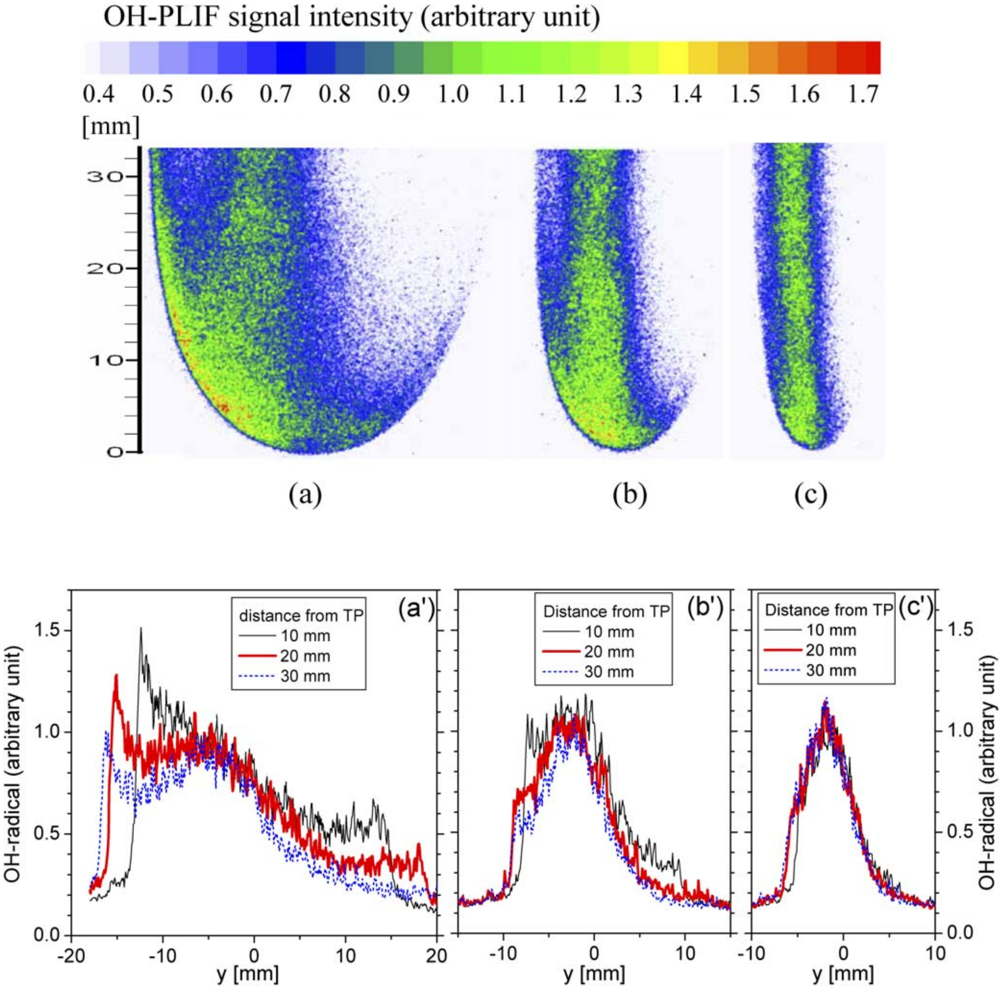

Fig. 11. The OH-PLIF signal and a comparison of the signal at the same distance from the flame base (propane, $V_{\mathrm{m},0} = 120$ cm/s); (a, a′) $V_\mathrm{f} = 101$ cm/s, $\nabla Y_{\mathrm{F,f}} = 0.0032$; (b, b′) $V_\mathrm{f} = 108$ cm/s, $\nabla Y_{\mathrm{F,f}} = 0.0081$; (c, c′) $V_\mathrm{f} = 105$ cm/s, $\nabla Y_{\mathrm{F,f}} = 0.0140$.

olution of less than 0.4% and can detect small effect of the diffusion flame if it has meaningful variation above 0.4%.

Second, the reaction rate along the diffusion branch was evaluated by measuring the OH radicals near the base of the flame in order to check the additional reaction. Fig. 11 shows the intensity of the OH-PLIF signal, and Figs. 11a′–11c′ show the distributions of the OH radical at three horizontal lines located 10, 20, and 30 mm from the base of each tribrachial flame. Since the PVTF values of the three cases have a similar order, the same horizontal distance from the flame base implies similar convective time scales. The OH radical usually has its maximum value along the diffusion flame and this phenomenon is evident in Figs. 11b′ and 11c′, similar result was observed by Won et al. [10].

When the concentration gradient was small, the maximum intensity was observed in the lean premixed branch, whereas the diffusion branch had a relatively weak intensity, as shown in Fig. 11a′. In addition, when the distance from the tribrachial point increased, the OH radical along the diffusion flame maintained almost the same value, whereas the OH radical of the premixed flame branch decreased. These results for the concentration gradient, which is smaller than the critical value, are similar to the trends of the experimental results of Kioni et al. [13], who observed dense OH radicals in the lean premixed flame branch. Additionally they reported the second peak increase in the OH signal in the direction of the stream along the diffusion flame. However, we found no renewed increase of OH radicals. Such a difference is likely caused by the difference in the fuel dilution.

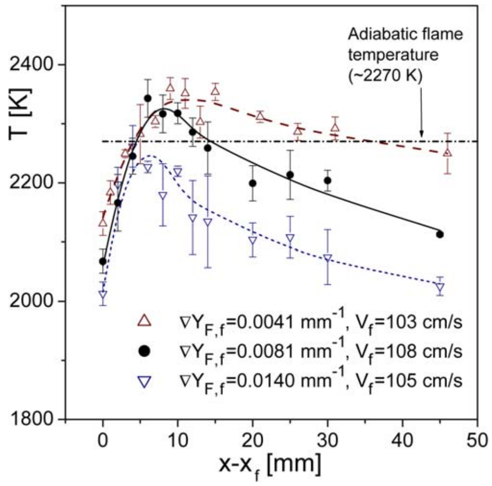

Fig. 12. Variation of the maximum temperature in the axial direction (propane, $V_{m,0} = 120$ cm/s).

In the case of Kioni et al. [13], fuel dilution increased the residence time along the diffusion flame branch, which could activate the contribution of the diffusion mechanism.

Finally, the temperature variation in the axial direction was measured using the CARS system by the space of 1 mm in horizontal direction (or y-direction). Fig. 12 shows the maximum temperature at the same height for three concentration gradients. The relative distance refers to the distance from where we measured the largest increase in temperature. Considering the probing space, it can be said that the temperature variation was steepest near the tribrachial point, while the maximum temperature was located slightly downstream.

When the concentration gradient is larger than the critical value, the maximum temperature decreases to a value that is less than the adiabatic flame temperature, and the peak of the maximum temperature is closer to the premixed branch. These results are typical of a tribrachial flame. While the concentration gradient was smaller than the critical value, the maximum temperature was slightly higher than the adiabatic flame temperature of the stoichiometric premixed flame. We also obtained such excess temperatures when the concentration gradients were sufficiently small in the open jet experiment [11].

Since the flame stretch effect is negligible at a sufficiently small concentration gradient, the gas temperature just behind the premixed flame approaches the adiabatic flame temperature theoretically. Then small disturbances concerned with the energy or species equations may cause additional temperature increase, and the following mechanisms can be suggested even though their estimation requires more study: (1) heat recirculation from the burned gas to the unburned mixture either by radiation through the gas phase or by conduction through the burner, which is enhanced by the size of the flame or total amount of the fuel consumption rate; (2) additional heat generation by the reaction along the diffusion branch coupled with the difference in various diffusion coefficients of heat and mass diffusion of abundant species such as O_2, CO, and H_2.

As the concentration gradient becomes smaller, the intensity of the luminosity and OH radicals of the diffusion flame decrease. Concerning the termination of the diffusion flame under the small concentration gradient, some studies have suggested that the effects of radiative heat loss from the gas phase are an important mechanism. Liu et al. [14] explained the extinction of the diffusion flame at a low stretch rate or low scalar dissipation rate, and Guo et al. [15] discussed the extinction of a premixed flame at a low stretch rate. They reported that the radiative heat loss from the gas phase participates in flame extinction, in addition to the main causes of convective and diffusive heat loss at the conditions close to extinction. And it was noted that the flame is extinguished not only by the global heat loss but also by the termination of chemical processes in such limit conditions.

Returning to the tribrachial flame in a channel, a similar situation may occur when the concentration gradient is small. Recently, Daou et al. [16] studied the effect of volumetric heat loss on the tribrachial flame, though their configuration differed from ours. Similar to their results [14–16], a diffusive reaction possibly has a low limit in the concentration gradient, and this concept will be applicable even for the edges of premixed flame branches. Such low limits of both the premixed flame and the diffusion flame may also play a significant role in the existence of the maximum PVTF. Such detailed investigation needed to fully elucidate the effect of the radiative heat transfer is, however, beyond the scope of this study.

4. Concluding remarks

In this experimental study, we examined the propagation velocities and characteristics of a tribrachial flame. In particular, we investigated the tribrachial flames in a slightly diverging channel to clarify the effect of a confined stream. The tribrachial flames in the confined channel had a maximum propagation velocity at a critical concentration gradient, and the critical concentration gradient increased to a larger value when the convective diffusion was enhanced. The propagation velocities in the channel were close to the flashback conditions of a tribrachial flame that has been stabilized in an open jet. As the concentration gradient increased, the growth of the diffusion flame branch was revealed by the distribution of the OH radicals using the PLIF method, and the growth of the diffusion flame branch was confirmed by temperature measurement using the CARS system. These results highlight the need to reconsider the role of the diffusion branch on the propagation velocity, especially under a confined (or squeezed) stream.

Acknowledgment

The authors are grateful for support from the Combustion Engineering Research Center at the Korea Advanced Institute of Science and Technology.

References

[1] H. Phillips, Proc. Combust. Inst. 10 (1965) 1277–1283.
[2] N. Ishikawa, Combust. Sci. Technol. 31 (1983) 109–117.
[3] J.W. Dold, Combust. Flame 76 (1989) 71–88.
[4] P.N. Kioni, B. Rogg, K.N.C. Bray, A. Liñán, Combust. Flame 95 (1993) 276–290.
[5] G.R. Ruetsch, L. Vervisch, A. Liñán, Phys. Fluids 7 (6) (1995) 1447–1454.
[6] Y.-C. Chen, R.W. Bilger, Combust. Flame 123 (2000) 23–45.
[7] S.H. Chung, B.J. Lee, Combust. Flame 86 (1991) 62–72.
[8] B.J. Lee, S.H. Chung, Combust. Flame 109 (1997) 163–172.
[9] Y.S. Ko, S.H. Chung, Combust. Flame 118 (1999) 151–163.
[10] S.H. Won, S.H. Chung, M.S. Cha, B.J. Lee, Proc. Combust. Inst. 28 (2000) 2093–2099.
[11] N.I. Kim, J.I. Seo, K.C. Oh, H.D. Shin, Proc. Combust. Inst. 30 (2005) 367–374.
[12] D.R. Snelling, R.A. Sawchuk, T. Parameswaran, Appl. Opt. 33 (1994) 8295–8301.
[13] P.N. Kioni, K.N.C. Bray, D.A. Greenhalgh, B. Rogg, Combust. Flame 116 (1999) 192–206.
[14] F. Liu, G.J. Smallwood, Ö.L. Gülder, Y. Ju, Combust. Flame 121 (2000) 275–287.
[15] H. Guo, Y. Ju, K. Maruta, T. Niioka, R. Liu, Combust. Flame 109 (1997) 639–646.
[16] R. Daou, J. Daou, J. Dold, Proc. Combust. Inst. 29 (2002) 1559–1564.